6. H. C. Brinkman, The viscosity of concentrated suspensions and solutions," J. Chem. Phys., 20, 571 (1952).
7. M. D. Millionshchikov, Turbulent Flow in the Boundary Layer and in Tubes [in Russian], Nauka, Moscow (1969).
8. M. D. Millionshchikov, "Turbulent flow in the boundary layer and in tubes," At. Énerg., 28, 207 (1970).

# NATURAL CONVECTION AND HEAT TRANSFER IN POROUS INTERLAYERS BETWEEN HORIZONTAL COAXIAL CYLINDERS

V. A. Brailovskaya, G. B. Petrazhitskii, and V. I. Polezhaev

UDC 536.25

## INTRODUCTION

It is known that in finely dispersed porous materials with communicating pores filled with a liquid or gas, large-scale (with respect to the pore sizes) natural convection arises under specific conditions, which can have a significant effect on the heat-insulating properties of these materials. Investigations of the average characteristics of the heat transfer through plane horizontal and vertical layers of porous material and a comparison of them with experimental data are performed in [1-4]. The effect of convection on heat transfer in porous annular interlayers, which are elements of many engineering constructions (heat insulation of the volume contents of pipes, cables, and so on), is numerically investigated in this paper. Heat transfer in the annular interlayers of compression electric furnaces has been investigated in [5, 6]. Investigations have been carried out in [7, 8] for homogeneous annular interlayers filled with a liquid or gas.

§1. An annular interlayer of finely dispersed isotropic porous material is formed by two horixontal coaxial cylinders on whose outer and inner surface are maintained the constant temperatures $T_2$ and $T_1$, respectively.

In order to calculate the flow field and heat transfer the convection equations are used in the Boussinesq approximation, and the surface-friction force is replaced by the equivalent volume drag force in accordance with Darcy's law [9]. For the steady-state convection mode this system has the form

$$\begin{gathered}\mu\mathbf{v}/k = -\nabla p + \rho g\beta\Delta T,\\ \operatorname{div}\mathbf{v} = 0,\quad \rho c_p(\mathbf{v}\nabla)T = \lambda^*\nabla^2 T,\end{gathered} \tag{1.1}$$

where $\rho$ is the density, $\beta$ is the volume expansion coefficient, $\mu$ is the dynamic viscosity coefficient, $\mathbf{v}$ is the velocity, $c_p$ is the specific heat of the gas or liquid filling the pores, $\lambda^*$ is the thermal conductivity of the porous medium without convection taken into account, p is the pressure difference from the static value, T is the mean temperature of the medium, $\Delta T$ is the difference between the local and some characteristic temperature, and k is the permeability coefficient of the porous medium.

Determining, as usual, the stream function $\psi$ by the relationships $u = \partial\psi/\partial y$, and $v = -\partial\psi/\partial x$ (u and v are the components of the velocity $\mathbf{v}$ on the x and y axes) and eliminating the pressure from the equations of motion (1.1), we write down in the polar coordinate system in dimensionless form the system of equations for the stream function and the temperature $\Theta$

$$\begin{gathered}\frac{\partial^2\psi}{\partial r^2} + \frac{1}{r}\frac{\partial\psi}{\partial r} + \frac{1}{r^2}\frac{\partial^2\psi}{\partial\varphi^2} = -\mathrm{Ra}^*\left(\frac{\partial\Theta}{\partial r}\cos\varphi - \frac{1}{r}\frac{\partial\Theta}{\partial\varphi}\sin\varphi\right),\\ \frac{\partial^2\Theta}{\partial r^2} + \frac{1}{r}\frac{\partial\Theta}{\partial r} + \frac{1}{r^2}\frac{\partial^2\Theta}{\partial\varphi^2} = \frac{1}{r}\left(\frac{\partial\psi}{\partial\varphi}\frac{\partial\Theta}{\partial r} - \frac{\partial\psi}{\partial r}\frac{\partial\Theta}{\partial\varphi}\right),\end{gathered} \tag{1.2}$$

where $\mathrm{Ra}^* = g\beta\delta k\rho^2 c_p\Delta T/\mu\lambda^*$ is the Rayleigh filtration number, which is the analogue of the Rayleigh criterion for a porous medium.

Gor'kii. Translated from Zhurnal Prikladnoi Mekhaniki i Tekhnicheskoi Fiziki, No. 6, pp. 90-96, November-December, 1978. Original article submitted November 16, 1977.

0021-8944/78/1906-0781$07.50  

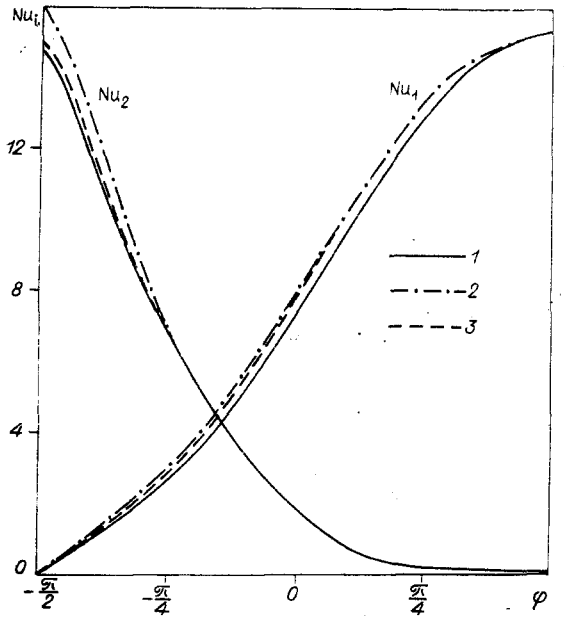

Fig. 1

The following quantities are selected as the scales for the reduction to dimensionless form: length scale $\delta = R_2 - R_1$, velocity scale $a^*/\delta$ ($a^* = \lambda^*/c_p\rho$), temperature scale $\Delta T = T_2 - T_1$, and pressure scale $\mu a^*/k$.

The boundary conditions are of the form

$$\left.\begin{aligned} &\psi = 0 \text{ at } r = r_1, r_2, \\ &\Theta = 0 \text{ at } r = r_1, \\ &\Theta = 1 \text{ at } r = r_2 \end{aligned}\right\} -\pi/2 \leqslant \varphi \leqslant \pi/2,$$

$$\partial\Theta/\partial\varphi = 0 \quad \text{at} \quad r_1 \leqslant r \leqslant r_2, \quad \varphi = \pm\pi/2.$$

The last condition indicates symmetry with respect to the vertical axis passing through the center of the region. This condition and the two-dimensional nature of the fields are the main assumptions which may not be satisfied for large values of Ra*. The determination of the range of applicability of these assumptions requires additional research.

§2. A finite-difference scheme for the numerical solution of the system (1.2) is set up by the balance method, which was applied earlier to the calculation of natural convection in homogeneous media [7, 8]. To this end each equation of the system is integrated over an elementary cell of a grid. The grid is introduced by the coordinates

$$r_i = r_1 + i\Delta r, \qquad i = 0, 1, 2, \ldots, l,$$
$$\varphi_j = -\pi/2 + j\Delta\varphi, \qquad j = 0, 1, 2, \ldots, m.$$

According to Green's equations, a portion of the two-dimensional integrals is converted into curvilinear integrals along the boundary of the cell, which are then replaced by finite sums. The remaining integrals are calculated according to the theorem of the mean, whereby the derivatives at the central point are obtained as the arithmetic mean values of the derivatives on the four sides of the cell. The steady-state solution of the system (1.2) is found by the build-up method with the help of iterations on some parameter analogous to the time.

A null field of the stream function $\psi(r, \varphi) = 0$ and a logarithmic temperature distribution between the heated and cold walls, which is characteristic for the thermal conductivity mode, are specified as the initial conditions.

The solution of the finite-difference equations is carried out according to the explicit scheme of the Seidel method [10]. The difference analogue of the system (1.2) has the form

$$z_{i,j}^{n+1} = z_{i,j}^{n} + \Delta\tau\Phi\left(z_{i,j}^{n};\ z_{i+1,j}^{n};\ z_{i,j+1}^{n};\ z_{i,j-1}^{n+1};\ z_{i-1,j}^{n+1}\right),$$
$$z_{i,j}^{n} = z(r_i,\ \varphi_j,\ \tau_n), \quad \tau_n = n\Delta\tau, \quad n = 0, 1, 2, \ldots,$$

where $\Phi$ is the difference operator of the system approximating (1.2).

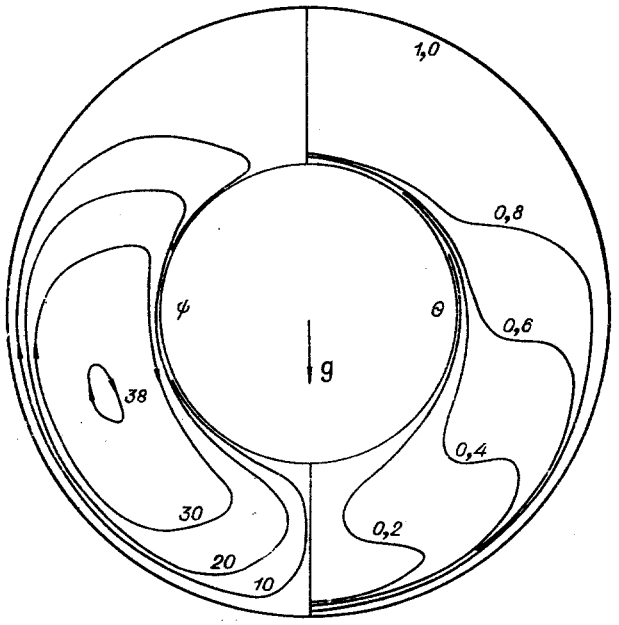

Fig. 2

The iteration step $\Delta\tau$ is selected from the stability conditions of the scheme, obtained by the Fourier method, and is corrected in the course of the actual calculations for different values of the Rayleigh criterion.

The numerical realization of the system of equations (1.2) possesses some specific properties, including a large sensitivity of the scheme to the grid parameters in comparsion with the case of the calculation of the convection of a homogeneous fluid [7, 8], which is produced by the characteristics of both the system (1.2) itself and the boundary conditions for the velocity field ($\partial\psi/\partial n \neq 0$, in contrast to [7, 8]).

The systematic calculations which were performed have permitted recognizing the essential grid parameters for producing sufficiently accurate solutions. The control of the accuracy of the calculations is accomplished by, in addition to a comparison of solutions with different grids, checking the discrepancies of the integral heat balances on the outer and inner surfaces of a layer. The main calculations were performed with a 22 × 22 difference grid and also with a 16 × 30 grid for one-half of the annular region in the case of relatively thin interlayers.

The results given below refer to the case $T_2 > T_1$ (the outer cylinder has a higher temperature). In the case in which the inner cylinder is heated, the temperature field is symmetrical with respect to the radial line ($\varphi = 0$).

The variation of the local Nusselt numbers $Nu_i(\varphi)$ along the outer ($i = 2$) and inner ($i = 1$) surfaces obtained with three different grids is shown in Fig. 1 ($Ra^* = 600$, $r_2/r_1 = 2$). The numbers $Nu_i$ are determined as dimensionless temperature gradients on the boundaries of the region and are approximated by three-point formulas of second-order accuracy within the region. As is evident from Fig. 1, the results are overestimated with a grid too coarse in radius, and the maximum discrepancy of the local thermal fluxes with the 17 × 17 (curve 3) and 16 × 30 (curve 2) grids compared with the results using a 22 × 22 grid (curve 1) amount to 10%.

§3. The typical pattern of steady-state motion and the temperature field in the region under discussion is shown in Fig. 2 ($Ra^* = 1000$, $r_2/r_1 = 2$). Natural filtration of the fluid in the porous medium occurs, as is evident from the pattern of the streamlines $\psi$ on the left in Fig. 2, as in a homogeneous medium along crescent-shaped trajectories upward along the heated outer wall and downward along the cold inner wall. A heated stagnation zone is formed in the upper part of the cavity, which is readily visible both from the patterns of the streamlines and from the isotherms on the right in Fig. 2. The temperature in the upper part of the cavity is higher, which causes heat transfer along the layer. As the Rayleigh filtration number increases, the strength of the convective flow and the temperature stratification increase, which leads for some Rayleigh numbers to the formation of regions with a reverse

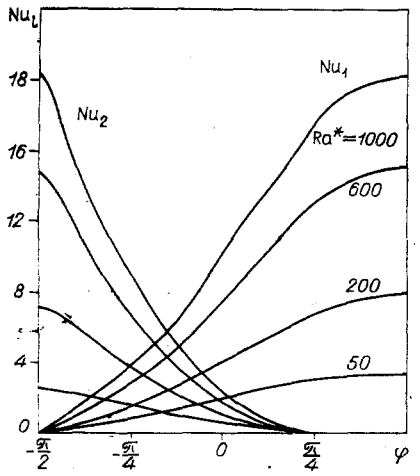


Fig. 3

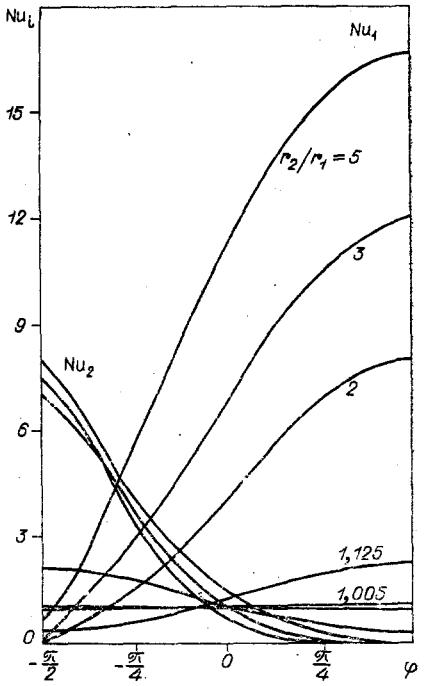


Fig. 4

temperature gradient. The temperature stratification exerts an appreciable effect on the development of boundary layers and, consequently, on the distribution of heat fluxes on the cold and heated surfaces. The distributions of local Nusselt numbers along the inner and outer boundaries of the region are given in Fig. 3 ($r_2/r_1 = 2$) for different values of the Rayleigh filtration number. The maximum local heat fluxes are realized at the initial section of the fluid flows washing over the cold and hot walls. As the thickness of the boundary layers increases, the local Nusselt numbers decrease, reaching values at $\varphi = \pi/2$ on the hot and $\varphi = -\pi/2$ on the cold surface which are less than the corresponding fluxes under conditions of pure thermal conduction. As follows from Fig. 3, this inequality of the thermal fluxes on the boundaries increases as Ra* increase. This tendency occurs upon an increase of $r_2/r_1$ (Fig. 4, Ra* = 200); therefore, information only on mean values of the convective heat transfer (<Nu> or $\varepsilon_c$) may be insufficient, for example, for the calculation of the heating up of construction elements protected by porous insulation.

The principal quantity being sought, which is of interest for engineering applications, is the convection coefficient $\varepsilon_c$, which is equal to the ratio of the mean heat flux through the interlayer when convection is present to the heat flux under conditions of thermal conductivity. The criterion equation for the convection coefficient is of the form

$$\varepsilon_{c_i} = \varepsilon_{c_i}(\mathrm{Ra}^*,\ r_2/r_1),$$

$$\varepsilon_{c_i} = \langle \mathrm{Nu}_i \rangle r_i \ln r_2/r_1, \quad i = 1,\ 2,$$

where

$$\langle \mathrm{Nu}_i \rangle = \frac{1}{\pi} \int_{-\frac{\pi}{2}}^{\frac{\pi}{2}} \left( \frac{\partial \Theta}{\partial r} \right)_i d\varphi.$$

The dependence of the convection coefficient on the Rayleigh filtration number is given in Fig. 5 for different values of the size of the gap width $r_2/r_1$. As in the case of convection in a homogeneous layer of liquid or gas [7, 8], one can distinguish three modes here: the thermal conductivity mode (small values of Ra*), an intermediate mode, and the boundary-layer mode.

The results of the analytic solution [5], which is valid for small Ra*, are denoted by the dashed lines in Fig. 5. The experimentally measured values of the convection coefficient [5, 6], obtained in permeable heat insulation (a filling of sand and graphite, $k \sim 1.3 \cdot 10^{-9}$ and $k \sim 8 \cdot 10^{-9}$ $m^2$, respectively) in a nitrogen and argon atmosphere at a pressure up to 130

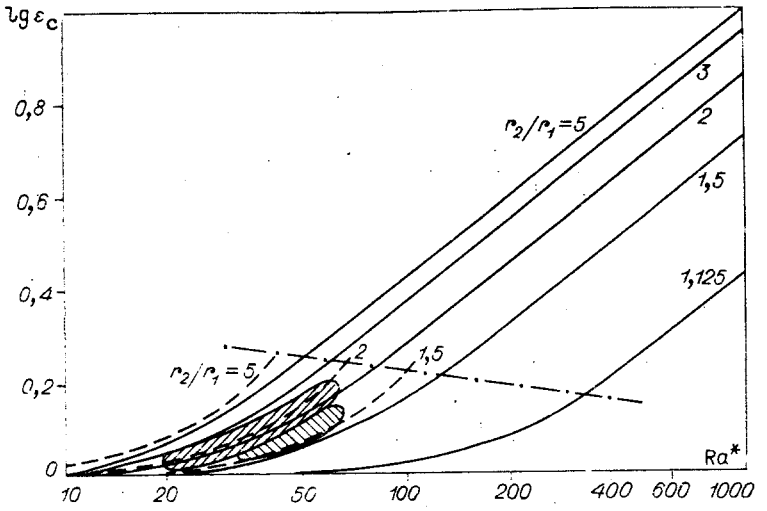

Fig. 5

TABLE 1.

| $r_2/r_1$ | 5 | 3 | 2 | 1,5 | 1,125 | 1,005 |
|---|---|---|---|---|---|---|
| $Ra_0^*$ | 12 | 14 | 20 | 37 | 100 | 2000 |

atm for two geometries of the annular layer ($r_2$ = 26.9 mm, $r_1$ = 13.5 mm and $r_2$ = 32.5 mm, $r_1$ = 17.5 mm), are shown (with scatter taken into account) by the crosshatched regions. For each $r_2/r_1$ relationship it is possible to determine the value of the Rayleigh filtration number $Ra_0^*$ starting from which the role of convection in the heat transfer becomes perceptible. The values of $Ra_0$ for which the convection coefficient differs from unity by 5% are given in Table 1.

In the boundary-layer mode (delineated by the dashed–dotted line) the dependence of the convection coefficient on the Rayleigh number is a power-law relation: $\varepsilon_c = c(Ra^*)^{0.57}$, and c is a function of the ratio of radii $r_2/r_1$ and has the form $c = 0.406(\log r_2/r_1)^{0.685}$ for $1.2 \leqslant r_2/r_1 \leqslant 3$.

The greatest variations of the convection coefficient are observed when $r_2/r_1$ varies within the interval $1.005 \leqslant r_2/r_1 \leqslant 2.5$; the larger Ra* is, the stronger is the effect of the radius ratio $r_2/r_1$ on the quantity $\varepsilon_c$. For relatively wide interlayers ($3 \leqslant r_2/r_1 \leqslant 8$), $\varepsilon_c$ is practically independent of the geometry.

Thus, the results of the numerical investigations shows that, just as in plane interlayers [2, 3], a distinctive feature of convection in annular porous interlayers (in comparison with the case of a homogeneous medium) is a stronger dependence of the mean thermal flux through the layer on the Rayleigh number and the geometry, as well as an appreciably greater inequality in the distribution of local thermal fluxes on the region boundaries.

The authors express their gratitude to V. L. Mal'ter for the use of his experimental data and for useful discussions of the results of this research.

LITERATURE CITED

1. M. Combarnous, "Convection naturelle et convection mixte dans une couche poreuse horizontale," Revue Générale de Thermique, 9, No. 108, 1355-1376 (1970).
2. M. P. Vlasyuk and V. I. Polezhaev, "Investigation of heat transfer in the case of natural convection in permeable porous materials," in: Heat and Mass Transfer [in Russian], Vol. 1, Part 2, Izd. Inst. Teplo- i Massoobmena Akad. Nauk BelorusSSR, Minsk (1972).
3. M. P. Vlasyuk and V. I. Polezhaev, Natural Convection and Heat Transfer in Permeable Porous Materials [in Russian], Preprint No. 77, Inst. Probl. Mekh. Akad. Nauk SSSR (1975).
4. Y. W. Elder, "Steady free thermal convection in a porous medium heated from below," J. Fluid Mech., 27, Pt. 1, 29-48 (1976).

5. V. L. Mal'ter, Z. M. Antropova, L. V. Petrova, and O. M. Kostenko, "Heat transfer in electrical resistance furnaces with high gas pressure," in: Research in the Area of Industrial Electrical Heating [in Russian], No. 4, Énergiya, Moscow (1970).
6. V. L. Mal'ter, V. N. Morozov, A. L. Pushkin, and O. M. Kostenok, "Calculation of convective heat transfer in lined furnaces with the use of a gas permeability coefficient," in: Electrical-Engineering Industry [in Russian], No. 7, Informélektro, Moscow (1974), p. 143.
7. G. B. Petrazhitskii, E. V. Bekneva, V. A. Brailovskaya, and N. M. Stankevich, "Numerical investigation of the flow and heat transfer in the case of the motion of a viscous heat-conducting compressible gas in a horizontal annular channel under the action of body forces," in: Transactions of the Second Republic Conference on Aerohydromechanics, Heat Transfer, and Mass Transfer [in Russian], Izd. Kievsk. Univ., Kiev (1971).
8. V. A. Brailovskaya and G. B. Petrazhitskii, "Thermal laminar convection of a fluid in an annular region with a specified heat flux," Zh. Prikl. Mekh. Tekh. Fiz., No. 3 (1977).
9. C. W. Horton and F. T. Rogers, "Convection currents in a porous medium," J. Appl. Phys., 16, 367-370 (1945).
10. I. S. Berezin and N. P. Zhidkov, Computational Methods [in Russian], Nauka, Moscow (1966).

# ANALYTIC DESCRIPTION OF BINARY MELT CRYSTALLIZATION

T. A. Cherepanova

UDC 536.42+536.421+518.517

In [1, 2] an approach was developed for the analytic description of the crystallization of binary systems. Diffusion processes at the interphase boundary were assumed to occur so intensely that the concentration in the melt was independent of the local phase-boundary configuration. Such an approximation is physically justifiable if the crystallization process is limited to its kinetic stage. In the case where the characteristic rate of diffusion mass transfer in the concentration boundary layer is less than the maximum possible growth rate at specified temperature values and specified component concentrations in the melt core, we must consider the crystallization process in a diffusion regime. The growth rate and structural characteristics of the interphase zone are then determined by diffusion mass transfer to the phase boundary and the value of the concentration gradient which develops near the boundary.

The purpose of the present study is an analytic description of the crystallization of binary melts with consideration of diffusion in the melt. With a microscopic examination of the kinetics of elementary process we will obtain a system of finite-difference equations for the diffusion boundary layer near the surface of the growing crystal faces.

We will consider a lattice model of the binary crystal–melt system. We assume that atoms of the $\alpha$ and $\beta$ components are located at lattice points and belong to either the liquid or solid phase. At each lattice point there is located only one such particle, the total number of which is equal to N. Interaction within the system will be described by the values of the effective binding energies of the most closely neighboring solid particles $\varphi_{11}^{\alpha\alpha}$, $\varphi_{11}^{\alpha\beta}$, $\varphi_{11}^{\beta\beta}$; of solid particles with liquid particles $\varphi_{10}^{\alpha\alpha}$, $\varphi_{10}^{\beta\beta}$, $\varphi_{10}^{\alpha\beta}$, $\varphi_{01}^{\alpha\beta}$; and of liquid particles $\varphi_{00}^{\alpha\alpha}$, $\varphi_{00}^{\alpha\beta}$, $\varphi_{00}^{\beta\beta}$ (the subscript 0 denotes the liquid phase, while the subscript 1 denotes the solid phase). As in [1, 2], the configuration of the distribution of atoms over the system is specified by a set of parameters $\mathbf{g} = \begin{Bmatrix} \xi_j \\ \eta_j \end{Bmatrix}$, where $\eta_j = 1$ if at the j-th lattice point a solid particle exists and $\eta_j = 0$ if a liquid particle is present; $\xi_j$ defines the type of particle at this point ($\xi_j = \alpha, \beta$). We denote by $\rho(\mathbf{g}, t)$ the probability of finding the system at time t in a state with configuration $\mathbf{g}$. The time evolution of the distribution function $\rho(\mathbf{g}, t)$ in our model is the result of completion of elementary events of transition of liquid

Riga. Translated from Zhurnal Prikladnoi Mekhaniki i Tekhnicheskoi Fiziki, No. 6, pp. 96-104, November-December, 1978. Original article submitted December 27, 1977.

 0021-8944/78/1906-0786$07.50 